International Journal of Industrial Electronics, Control and Optimization © 2022 IECO
Vol. 5, No. 2, pp. 143-151, April (2022)

# Design and Implementation of a Novel Wind Turbine-PMSG for Marine and Domestic Water Purification Application

Hassan Zare[1, †], Alireza Nateghi[2], Hossein Asgharpour-Alamdari[3], Mohsen Latifi[4]

[1,3]Department of Electrical Engineering, Technical and Vocational University (TVU), Tehran, Iran.
[2]Faculty of Electrical and Computer Engineering, Shahid Sattari University of Aeronautical Engineering, Tehran, Iran.
[4]Faculty of Electrical and Computer Engineering, Islamic Azad University, Tehran, Iran.

**ABSTRACT**

*The supply of purified water in marine and domestic applications, especially in remote areas regarding fossil fuels environmental pollutants, makes it hard to use conventional energy sources. Therefore, the present research seeks to construct a water purification system by using reverse osmosis technology supplied by a novel wind turbine driven with a permanent magnet synchronous generator. To reach this goal, an efficient high torque wind turbine was designed with new butterfly blades in which the lift and drag forces were determined along with creating twisting angles in blades. The blades were initially designed in SolidWorks software. Then, the computational fluid dynamics principles were simulated in the COMSOL5.2a environment by utilizing the k-ω pattern and multi-reference coordinate axis method. A laboratory prototype was implemented to verify the theoretical calculations, simulation analysis, and validity of the wind turbine. To ensure the sufficient capability of the system in worse situations, the performance of the turbine system at a low wind speed of 4 m/s was evaluated. The results showed that a maximum power factor of 0.29 was obtained, making the micro-turbine appropriate for both marine and domestic sweetener systems.*

**Article Info**

***Research Article***
***Keywords:***
Desalination System, PMSG, Reverse Osmosis, Savonius, Wind Turbine.
***Article History:***
**Received** 2021-10-13
**Accepted** 2022-04-04

## I. INTRODUCTION

Nowadays, access to adequate purified water is turning into a global issue given the growing expansion of human societies and industrial development [1]. On the other hand, increasing concern about generating electricity from fossil energy due to their depletion crisis and environmental pollutant emissions necessitated energy generation from renewable energy sources [2]. Among all sorts of emerging energies, wind power has a special place due to lower energy costs, high efficiency, easy access, and eco-friendliness, which has attracted the attention of many researchers and industrialists [3]. It is anticipated that by 2050, at least 12% of the world's electrical energy will be generated from wind. Wind turbines operate on the basis of a drag force like an open sail, and the wind force pushes the desired surface [4]. Savonius Rotor is a very simple example of the windmill based on the drag force [5]. These turbines move because the drag force in the open and concave regions of these rotors is much larger and more than that in the closed and convex regions. In these turbines, the drag force acts as a propulsion force to rotate the blades. Savonius turbines usually have two or three wind power absorption blades. The design of these turbines is such that the rotational speed is low, but a large torque is generated in each turning circle. Studies on the aerodynamic behavior of the Savonius blade to increase its efficiency have suggested that the height of the blade will be considered twice its diameter, the initial overlap ratio will be between 0.15 and 0.3, and the second overlap distance will be zero

[†]**Corresponding Author**: hszare@tvu.ac.ir
Tel: +98-1144730114, Technical and Vocational University
Department of Electrical Engineering, Technical and Vocational University (Tvu), Tehran, Iran

Copyright © 2022 Zare et al. Published by University of Sistan and Baluchestan. This work is licensed under a Creative Commons Attribution-Noncommercial 4.0 International license. (https://creativecommons.org/licenses/by-nc/4.0/). Non-commercial uses of the work are permitted, provided the original work is properly cited

[1, 5]. Besides, analyzing the helix rotor in comparison with its power production, torque, start-up characteristics, and rotational speed with conventional Savonius and their work results show higher efficiency and easier startup compared to conventional Savonius [6]. In addition, an experimental study on the Savonius turbine found that with the increase in the speed coefficient of the blade tip, the efficiency of these turbines increased, and the turbine with an overlapping space β and a round at the ends of the plates had better performance than the turbine without them [7]. The advantages of Savonius turbines for domestic electricity generation and wind turbine efficiency at various speeds were studied in [8]. The position of blades against the wind was investigated by [9] in an experimental and numerical study on a small type Savonius wind turbine. Aerodynamic simulation of a Savonius micro-turbine was conducted in [10] to identify the suitable point for installing wind turbines on the roof of a solar building. The effects of the overlapping ratio on the performance of domestic wind turbines were examined both numerically and experimentally in [11] according to which the best overlap ratio for this rotor is 20%. Authors in [12] tested wind turbines for quantitative and qualitative drinking water production by using RO systems in Ghana. In [13], a sweetener system was designed using wind turbines for rural areas to facilitate maintenance and allow high cost savings. An RO system with a back and forth pump that needed about 2 kW of power was utilized. Similarly, in [14], a study was conducted on the use of RO desalinating systems in a concrete plant. In this research, a comparative study was carried out to evaluate electrical energy versus wind energy for use as an energy source in RO desalinating systems.

On the other hand, Nuclear Energy Agency and Energy Information Management's report considered the equalized cost of power generation technologies in different countries as well as mentioning wind power as one of the cheapest power generation options [15]. Accordingly, many interesting solutions have been proposed for using wind power. The feasibility of using a Savenius wind micro-turbine on the roof of residential buildings was investigated in [16]. Similarly, many studies have been carried out on the use of Sovenius wind turbines in various applications. But, technical optimization of these turbines and their use in power generation for desalinating have been neglected. Therefore, the present study investigates the optimization of the Sovenius blade regarding the economic analysis of its application for electricity generation for a desalinating system. On the scale of domestic water consumption, reverse osmosis (RO) water desalination systems can only be used with wind power and without the need for another source because the electricity they need can be supplied by a small wind turbine and in the low-speed wind condition. The first step in the construction and installation of these small wind turbines is to conduct feasibility studies to assess the technical, economic, and infrastructural feasibility of establishing a water purification system using wind energy on a specific site using wind turbines. The rest of the paper is structured as follows: Section II introduces comprehensive modeling of the proposed system, including conventional units, electrical components, and Permanent Magnet Synchronous Generator (PMSG), as well as mechanical parts. Additionally, the model proposed for designing blades for an RO system incorporating a wind turbine is implemented in this section considering a detailed comparison between research samples. Section III presents the numerical results and simulation analyses obtained from the computational software. Section IV reports the experimental results derived from mechanical and electrical tests. Finally, the conclusions are summarized in Section V.

## II. Problem Description

### A. Governing equations of the fluid flow

Equations governing the flow of incompressible fluids are called Navier-Stokes equations. Many models have been suggested to solve these equations under different fluid conditions, each of which is suitable for a particular situation and its particular conditions. The fundamental equations in the analysis of fluids are the two relationships of conservation of mass (Eq. 1) and the relation of momentum (Eq. 2). Since there is a fluid rotation in the analysis of wind turbines, the two resultants, which are named Coriolis and centrifugal acceleration, are entered into the momentum equation. The Coriolis acceleration is defined as $2\vec{\omega} \times \vec{V_r}$ and the centrifugal acceleration as $\vec{\omega} \times \vec{\omega} \times \vec{r}$ where $r$ is the radial position of the rotation domain relative to the center, ω is the angular velocity of the spinning domain, $Vr$ is the relative velocity, $\rho$ is the static pressure, $\tau_r$ is the stress tensor, and F is the external forces subjected on the object [17].

$$\frac{\partial \rho}{\partial t} + \nabla . \rho \vec{V_r} = 0 \tag{1}$$

$$\frac{\partial}{\partial t}\left(\rho \vec{V_r}\right) + \nabla . \rho \vec{V_r} \vec{V_r}) + \rho\left(2\vec{\omega} \times \vec{V_r} + \vec{\omega} \times \vec{\omega} \times \vec{r}\right) = -\nabla \rho + \nabla \tau_r + \vec{F} \tag{2}$$

### B. Standard method k-ω

To simulate two flow domains, including rotors and stators, a combination of two Cartesian and cylindrical

coordinates was used. The standard k-ω model whose relations are presented in the following equations was used to analyze the turbulent flow [3]. These relationships are related to Navier Stokes relations by the flow switching parameters. The k-ω method is a suitable precision method for analyzing turbulent flow and Reynolds stresses caused by it.

$$\rho(u.\nabla)k = \nabla[(\mu + \mu_T\sigma_k)\nabla k] + P_k - \beta_0\rho\omega k$$
$$\rho(u.\nabla)\omega = \nabla[(\mu + \mu_T\sigma_\omega)\nabla\omega] + \alpha\frac{\omega}{k}P_k - \rho\beta_0\omega^2 \quad (3)$$

$$\mu_T = \rho\frac{k}{\omega} \quad (4)$$

$$P_k = \mu_T[\frac{\nabla u}{\nabla u + (\nabla u)^T}] \quad (5)$$

### C. Permanent Magnet Synchronous Generators

Permanent magnet synchronous generators (PMSGs) are kinds of synchronous generators that are connected to the system directly. However, higher reliability, efficiency, and power-to-weight ratio make them more attractive than other generators. Particularly, PMSGs are praised for direct drive, operating without a gearbox, slow rotation speed, and lack of rotor current. However, they still have some drawbacks. For example, they need an electromagnetic field with a flexible structure, which leads to high manufacturing and operation standards, and some temperature-related issues make them less applicable at wind farms.

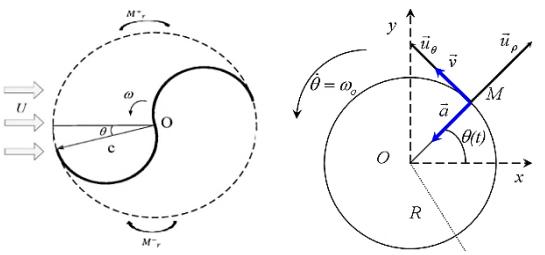



**Fig. 1.** The k-ω method for Sovenius wind turbine blade.

The high efficiency and low maintenance will reduce the cost, which is the most important concern to invest [18]. Further details about control systems, aggregation methods, and equivalent models for PMSG wind turbines are presented in [19]. Figure 2 describes the components of a PMSG system including the generator and grid side converters' controllers.

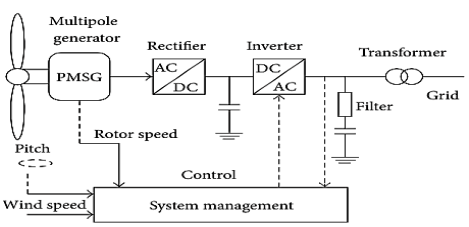



**Fig. 2.** A schematic of a wind turbine driven PMSG

Considering $\rho$ as air density in kg/m$^3$, blade pitch angle ($\beta$), $A_r$ as blade impact area in m$^2$, and wind speed in m/s ($V_w$), the power coefficient of the variable speed wind turbine ($C_p$), tip speed ratio ($\lambda$), and mechanical power ($P_m$) can be calculated as [2, 20]:

$$P_m = 0.5.\rho.A_r.V_w^3.C_p(\lambda,\beta) \quad (6)$$

$$C_p(\lambda,\beta) = 0.22 \times (\frac{116}{\gamma} - 0.4.\beta - 5).\exp(\frac{12.5}{\gamma}) \quad (7)$$

$$\frac{1}{\gamma} = \frac{1}{\gamma + 0.89} - \frac{0.035}{\beta^3 + 1} \quad (8)$$

$$\lambda = \frac{R.\omega}{V_w} \quad (9)$$

Further details and expressions are discussed in [21]. The relationship between mechanical power, torque, and wind speed can be established below:

$$T_m = \frac{P_m}{\omega} \quad (10)$$

Accordingly, the mechanical torque depends on the wind speed and regarding system states (6) to (10), the model of the wind turbine can be modeled. Hence, the Simulink platform of a wind turbine is shown in Fig. 3.

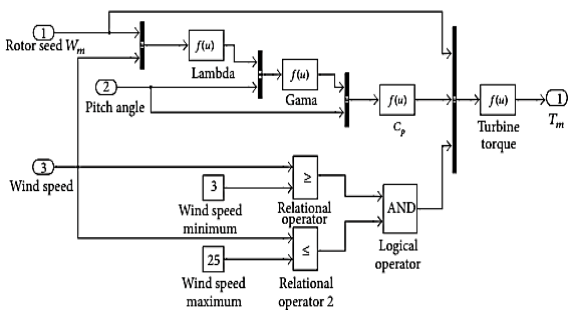



**Fig. 3**. The block diagram of the wind turbine aerodynamic.

The current equations for the generator with the help of a rotor-fixed rotating coordinate system can be calculated as follows:

$$\frac{di_{sd}}{dt} = -\frac{R_{sa}}{L_{sd}}i_{sd} + \omega_s\frac{L_{sq}}{L_{sd}}i_{sq} + \frac{1}{L_{sd}}u_{sd} \quad (11)$$

$$\frac{di_{sq}}{dt} = -\frac{R_{sa}}{L_{sq}}i_{sq} - \omega_s(\frac{L_{sd}}{L_{sq}}i_{sd} + \frac{1}{L_{sq}}\psi_p) + \frac{1}{L_{sq}}u_{sq} \quad (12)$$

Ultimately, the electromagnetic torque of the rotor is:

$$T_e = 1.5\frac{P}{2}\left[\psi_p i_{sq} + i_{sd}i_{sq}(L_{sd} - L_{sq})\right] \quad (13)$$

where $i_{sd}$ and $u_{sd}$ are the current and voltage of $d$-axis, respectively. Similarly, $i_{sq}$ and $u_{sq}$ are the q-axis current and voltage, $L_{sd}$ and $L_{sq}$ are the generator inductance, $\omega_s$ is the generator's electrical angular frequency, $\psi_p$represents the permanent flux, $R_{sa}$ represents the stator's resistance, and finally, $P$ is the number of the generator's poles.

### D. Reverse osmosis water purification method

Reverse Osmosis (RO) is a filtration method with membrane technology that eliminates many types of large

molecules and ions from the solution by compressing the solution behind the membrane. As a result, the solvents remain on the side under pressure, and the pure solvent is allowed to pass to the other side. If a semi-permeable membrane is placed between two solutions with different concentrations, some of the solvent is transferred from one side of the membrane to the other. The natural direction of the solvent movement (i.e., from a higher chemical potential to lower chemical potential) is in such a way that the more concentrated solution is diluted. Pure water passes through the membrane and enters saline water. If the system is allowed to reach a balance, then the level of more concentrated saline water will rise upper than the level of pure water. This difference in the surface on both sides of the membrane is called osmotic pressure. By applying more mechanical pressure than osmotic pressure to saline water, water molecules are separated from the salt molecules and the water moves towards the pure water section, which is called "reverse osmosis".

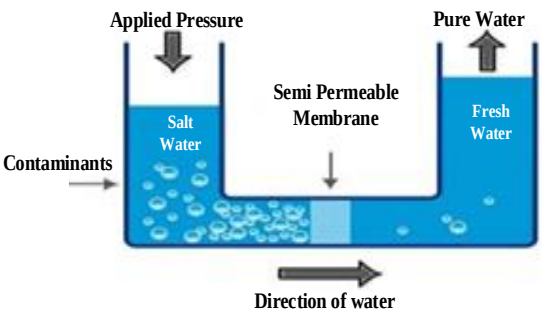



**Fig. 4.** Reverse Osmosis filtration overview.

*E. Comparison between research samples*

It is worth mentioning that the geometric and aerodynamic shape of the blade is the most important parameter in the operation of wind turbines, but limited research has been carried out in this field. Since one of the design goals in this research is to determine the effect of the aerodynamic shape of the blade on the efficiency and torque of wind turbines, a few examples of existing blades that have been investigated so far have been gathered in Fig. 5 and their properties have been investigated.

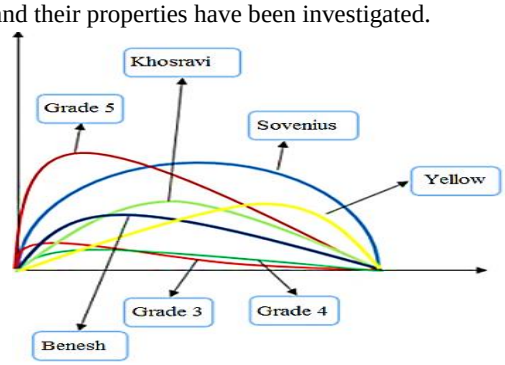



**Fig. 5.** Different geometric and aerodynamic shapes.

As can be seen, in all of these patterns, it has been tried to determine the effect of each of these parameters on turbine performance by increasing and decreasing the curvature of the blade. If the Benesh blade is considered a control blade, then the curvature of yellow, grade 3, and grade 4 patterns is lower and the curvature of Sovenius, Khosravi, and Grade 5 is higher than that of the Benesh blade [20]. Considering this point, the optimized turbine in this study has a higher power factor or better efficiency than the conventional Sovenius and Khosravi blades, but it has a lower power factor than the Benesh. Table I shows the lift ($L_C$) and drag coefficients ($D_C$) for several samples of turbine blades. It should be noted that in this table, Pc represents the center of pressure. As can be seen, the difference between the values of drag coefficients is not significant. On the other hand, the lift coefficients include a range of variables. Therefore, the most important factor in varying the efficiency of wind turbines of this type is the variation in the lift coefficient. For example, the conventional Sovenius turbine has the lowest lift coefficient and the lowest efficiency in the reports. Moreover, the length of the torque arm plays an important role in determining the efficiency of turbines, but not the most important factor, since the Benesh and conventional Savenius blades have the highest effective arm length, while they have the highest and lowest efficiency in the table, respectively.

**TABLE I**

THE COMPARISON OF POWER COEFFICIENTS AND DRAG AND LIFT FORCES OF DIFFERENT TURBINE BLADES.

| Blade name | Dc | Cp,max | Cm,max | Pc (cm) | λmax | Lc |
|---|---|---|---|---|---|---|
| Grade 5 | 3.01 | 0.34 | 0.41 | 9.3 | 1.3 | 0.07 |
| Grade 4 | 3.01 | 0.3 | 0.39 | 10.5 | 1.2 | 0.09 |
| Grade 3 | 3 | 0.31 | 0.4 | 10.5 | 1.2 | 0.11 |
| Benesh | 3.01 | 0.37 | 0.34 | 11.9 | 1.2 | 0.08 |
| Yellow | 3.08 | 0.36 | 0.34 | 10.8 | 1.2 | 0.11 |
| Khosravi | 3.16 | 0.26 | 0.29 | 10.6 | 0.9 | 0.007 |
| Sovenius | 2.3 | 0.23 | - | 11.9 | 0.8 | 0.001 |

## III. SIMULATION RESULTS

The equations mentioned for the wind turbine are solved by producing nodes in the control volume, the meshing method, and the quality of the produced meshes. Hence, three different models of turbines are designed, modeled, meshed, and analyzed in COMSOL software in this study. The specifications of this meshing are presented in Table II and the related meshing is illustrated in Fig. 6. In this study, the air fluid enters the computing region at a speed of 4 m/s. Either one of the two conditions can be used: input velocity and input flow, which do not have any difference as the fluid in the input has constant properties. The velocity input boundary conditions were used as well.

The output pressure boundary condition as zero we used, as well as the other walls, the floor and the ceiling of the computational area were determined by wall boundary conditions (see fig. 7).

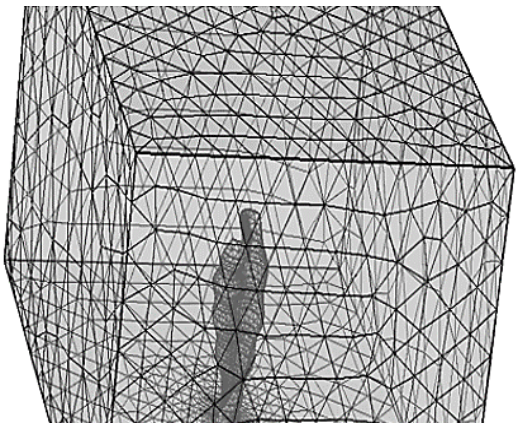


**Fig. 6.** The meshing of this study.

**TABLE II**
MESHING CHARACTERISTICS.

| Mesh types | Mesh numbers |
|---|---|
| In apexes | **36497** |
| Pyramid | **165530** |
| Tetrahedral | **2201** |
| Hexagonal | **89634** |
| Foursquare | **440** |
| Triangular | **9434** |
| In boundary layer | **18000** |
| In edges | **14870** |
| Total meshes | **337706** |
| Mesh quality | **0.4276** |

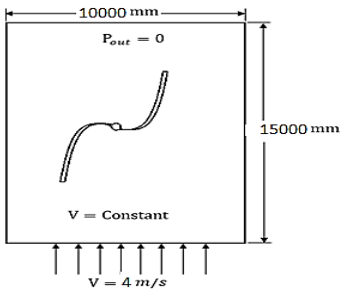



**Fig. 7.** Specific boundary conditions of this study.

According to the literature review, the potential of wind energy is calculated to be in the range of 900-1500 W/m$^2$. Therefore, the power of wind energy in the geographical regions of the country should be considered independently and regionally [20]. Hence, statistical methods, mathematical and computational relations, the amount of energy, and wind speed in different months are calculated in this research. For this purpose, daily and hourly statistics (eight times measured at three-hour intervals) for wind speed during the last 5 years of the synoptic meteorological station as presented in table III are used. Figure 8 shows the diagram of the pressure distribution on the simulated rotor surface, in which, according to the colors, the highest pressure on the turbine blade is at the rotor's edges and shows that with the flow of air into the airfoil-shaped blades, the airflow creates a lift force that causes the turbine to rotate. When the blades rotate 90° from the horizontal position, the blade profiles become completely tensile (preventer). The opening cup at the top causes the blade to rotate clockwise, while the downward cup is subjected to a preventing force, which is opposed to the blade rotation. In terms of blade shape, the purer torque is in the clockwise direction.

**TABLE III**
AVERAGE MONTHLY AND HOURLY WIND SPEED AND ITS PERCENTAGE VARIABILITY OF METEOROLOGICAL STATION

| Month | Wind speed (m/s) for each time period | | | | | | | | Average |
|---|---|---|---|---|---|---|---|---|---|
| | 0:00 | 03:00 | 06:00 | 09:00 | 12:00 | 15:00 | 18:00 | 21:00 | |
| **Jan** | 0.419 | 0.516 | 0.968 | 2.258 | 2.451 | 1.032 | 0.968 | 0.367 | **0.12** |
| **Feb** | 0.414 | 0.517 | 1.517 | 3.034 | 2.759 | 1.448 | 0.379 | 0.62 | **1.34** |
| **Mar** | 0.903 | 1.226 | 2.645 | 3.064 | 3.742 | 1.839 | 2.194 | 1.129 | **2.09** |
| **Apr** | 1.4 | 1.034 | 1.433 | 1.533 | 2.967 | 2.933 | 1.633 | 0.7 | **2.08** |
| **May** | 0.161 | 0.193 | 2.323 | 2.870 | 4.032 | 4.355 | 1.806 | 1.097 | **2.10** |
| **Jun** | 1.733 | 1.433 | 3.133 | 4.3 | 4.161 | 3.933 | 3.333 | 1.633 | **2.99** |
| **Jul** | 1.419 | 0.839 | 2.163 | 3.064 | 2.741 | 3.258 | 2.645 | 2.387 | **2.38** |
| **Aug** | 1.290 | 0.516 | 3.161 | 2.548 | 2.129 | 4 | 1.156 | 1.354 | **2.06** |
| **Sep** | 0.5 | 0.433 | 1.933 | 2.333 | 2 | 0.533 | 0.3 | 0.667 | **1.08** |
| **Oct** | 0.451 | 0.580 | 1.516 | 2.129 | 1.580 | 0.935 | 0.419 | 0.516 | **1** |
| **Nov** | 0.433 | 0.433 | 0.366 | 1.5 | 1.833 | 0.548 | 1.516 | 0.733 | **1.05** |
| **Dec** | 0.545 | 0.387 | 1.193 | 1.645 | 1.064 | 0.345 | 0.419 | 0.741 | **0.76** |
| $\bar{V}$ | 0.805 | 0.676 | 1.946 | 2.329 | 2.621 | 2.096 | 1.396 | 0.995 | **1.67** |
| $\sigma$ | 0.52 | 0.38 | 0.95 | 0.8 | 0.97 | 1.5 | 0.98 | 0.57 | **0.7** |
| $C_v$ | 64.5 | 55.5 | 48.9 | 34.7 | 37.3 | 71.9 | 70 | 57.4 | **41.7** |

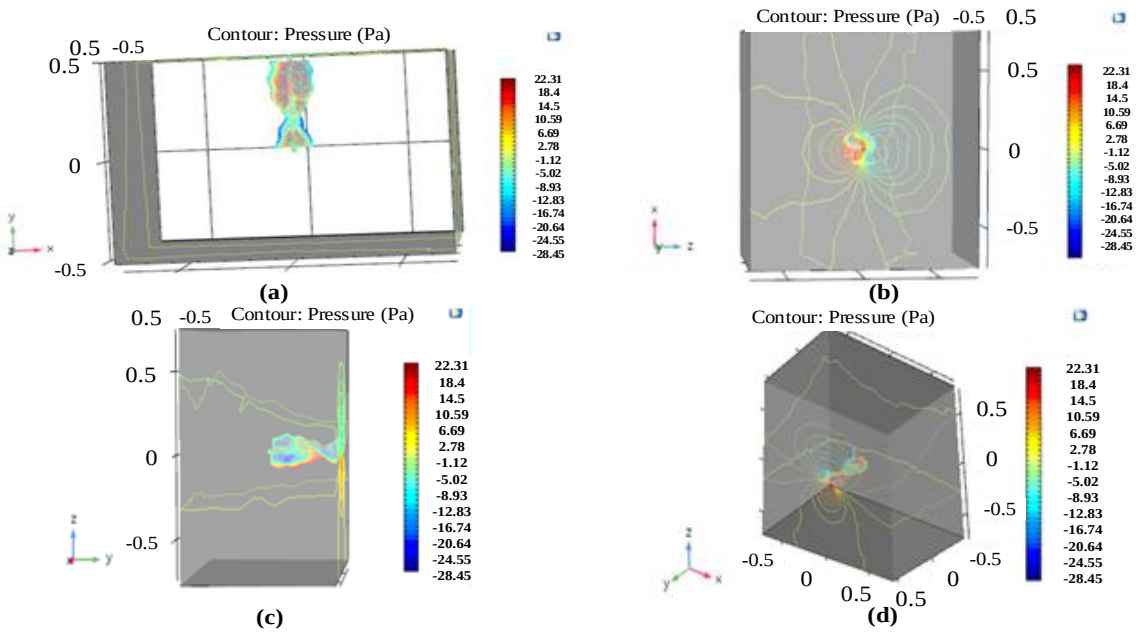



**Fig. 8.** Pressure distribution diagram **a**) in x-y, b) in x-z, c) in z-y and d) 3-dimensional

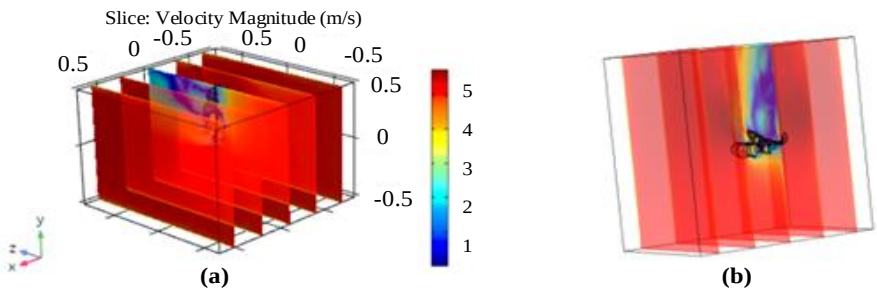



**Fig. 9.** Velocity distribution diagram a) of the turbine rotor and b) on the studying blade.

Since these two cups are connected by a middle portion, this causes the air to flow between the two blades and, as a result, reduces turbulence. Figure 9 shows the distribution of velocity on the turbine rotor and turbine blade, respectively. As seen in the figures, the maximum velocity is in the direction in which the wind hits the turbine rotor from ahead. To maximize the efficiency of the Sovenius rotor, the end plates should be used on both sides of the rotor. A part of the air fluid, after collision with the rotor, moves away from the rotor towards the rotor's edges so that the maximum momentum of the wind is not transmitted to the rotor and the efficiency decreases. The other thing is that the air fluid after colliding to the surface that faces wind rotation by 90° from the concave side moves upward and down the blade. In order to obtain the most momentum in its ideal state, this angle should increase to 180°. Figure 10 shows the power factor diagram based on the speed of the tip of the blade (m/s). The maximum power factor of 0.29 for the rotor's blade at the speed coefficient of 0.8 is obtained. Moreover, the lift and drag forces and the pressure center of the Sovenius blade at the Reynolds number range of 106 are obtained through simulations. Obtaining the center of pressure is necessary since the torque arm increases by increasing the distance between the pressure center and turbine center, thereby increasing the torque probability. Further simulation results are presented in Table IV. After determining the aerodynamic shape and the lift and drag forces, the torque f blades is obtained in a complete cycle using the CFD analysis.

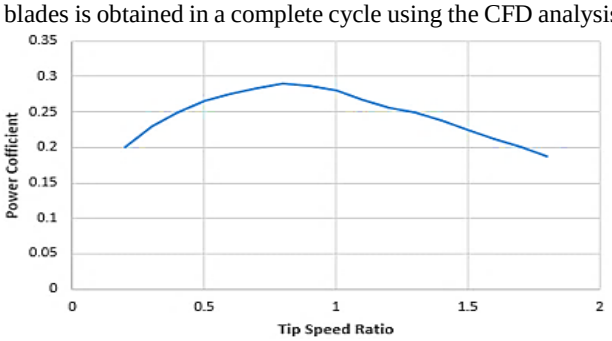



**Fig. 10.** PF diagram in terms of the tip of the blade speed (m/s).

**TABLE IV**

AERODYNAMIC CHARACTERISTICS OF THE ROTOR

| Parameter | Magnitude |
|---|---|
| Drag coefficient | 2.48 |
| Lift coefficient | 0.25 |
| Center of pressure (cm) | 12.72 |
| Average torque (N. m) | 22.27 |

Figure 11 indicates the torque subjected to the blades in a complete cycle. Accordingly, the maximum torque for the proposed turbine blades is 24.94 N.m, which is at 90°. To maximize the efficiency of the Sovenius rotor, the end plates should be used on both sides of the rotor. A part of the air fluid moves away from the rotor towards the rotor's edges after collision with the rotor so that the maximum momentum of the wind is not transmitted to the rotor, and thus, its efficiency decreases. To avoid this issue, it is necessary to use the end plates on the rotor. The other thing is that, similar to the previous section, the air fluid rotates 90° from the concave side after colliding with the surface in its ideal state and this angle should increase by 180°.

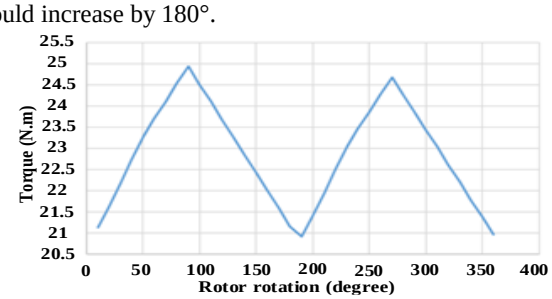



**Fig. 11**. The torque diagram subjected to the blade.

## IV. EXPERIMENTAL RESULTS

The executive activity for blade metrology (metallurgical and mechanical properties) is obtained by comparing the strength and flexibility of the aluminum alloy sheets to other steel and foam sheets. As a result, aluminum alloy is chosen in this study. After that, regarding the design, each blade is divided into five equal parts. In this case, if a part of the blade is damaged, it can be easily replaced and the maintenance costs would be reduced. In the next step, these blades are cut by laser and then curved with a working roll that has a radius of 0.46 m for the turbine blade, which is less than the radius of conventional Savonius wind turbines. This feature results in a greater force and torque on the blades and greater power for the turbine. Then, by coupling the wind turbine and the generator, the proposed setup was structured. Moreover, the MRO1644 water desalination system is utilized in which the amount of sweetened water is 187 L/day. Due to the DC 30 w/hrs power demand of the device, a PWM rectifier was applied in. Accordingly, the properties of the test system are presented in Table V and the photo of the setup in the test environment including both the wind tunnel and suppling the water desalination system is illustrated in Fig. 12. As a result, the experimental results are summarized in Table VI, approving the sufficient perfomance of the system and satisfying the required power demand during every possible condition as considered during system design.

**TABLE V**

PROPERTIES OF THE LABORATORY PROTOTYPE

| Name | Vertical Axis Wind Turbine |
|---|---|
| Started Wind Speed | 1 m/s |
| Rated Wind Speed | 10 m/s |
| Safe Wind Speed | 45 m/s |
| Rated Voltage (DC) | 12.24 v |
| Rated Power | 100 watt |
| Max Power | 150 watt |
| Rotor Diameter of Blades | 0.48 m |
| Blades Height (m) | 1 m (include generator 8 flange) |
| Blades Material | Aluminum Alloy |
| Generator | PMSG |
| Work Environment Temperature | -10 $c^o$ ~ +40 $c^o$ |
| Work Environment Humidity | Controller and inverter ≤ 80% |
| Product Assembly Weight (kg) | < 19 kg |



a) b)

**Fig. 12.** The overview of the manufactured laboratory prototype for a) wind tunnel test and b) RO application.

**TABLE VI**

EXPERIMENTAL RESULTS OF THE PROPOSED STRUCTURE

| Torque (N.m) | Power (watt) | Current (A) | Voltage (Volt) | Angular Speed (rad/sec) |
|---|---|---|---|---|
| 5.94 | 19.62 | 1.8 | 10.9 | 200 |
| 7.30 | 36.5 | 2.5 | 14.6 | 300 |
| 6.54 | 43.21 | 2.9 | 14.9 | 400 |
| 7.42 | 61.6 | 4 | 15.4 | 500 |
| 8.30 | 83.04 | 4.8 | 17.3 | 600 |
| 8.38 | 97.24 | 5.2 | 18.7 | 700 |
| 8.65 | 115.05 | 5.9 | 19.5 | 800 |
| 8.39 | 125.86 | 6.2 | 20.3 | 900 |

## V. CONCLUSION

This study aimed to design, simulate, and manufacture the rotor of wind turbine CH-50/butterfly type and use it as a power generator for a water desalinating system. To achieve this goal, the aerodynamic performance of this blade was first calculated by using computational fluid dynamics and performing 3D simulations. Both of the simulation results and analyses demonstrated 0.29 for the power coefficient of the rotor at a speed coefficient of 0.8. Also, the rotor has a torque of 24.94 N.m at 90 in a complete cycle. Comparing the two-dimensional analysis of simulations demonstrated

that the difference between the wide range values of lift and drag coefficients was not significant. The highest drag coefficient was for a blade that had a low lift factor. Therefore, the lift coefficient variations can be considered the most important factor in the efficiency variations of this turbine type. Besides, the length of the torque arm plays an important role in determining the efficiency of the turbines. At last, a prototype test setup was implemented and the various tests regarding the technical specifications of the desalination system were conducted. The results indicate that the amount of the generated power by the proposed setup can meet the demand of the desalination system, leading to providing 187 liters of purified water per day.

## REFERENCE


[1] A. Khajeh & Z. Shabani, Adaptive gain scheduling control of doubly fed induction generator based wind turbines to improve fault ride through performance. *International Journal of Industrial Electronics, Control and Optimization*, 1(1), 61-70, 2018.

[2] R. Zeinali & M. Salehi, The Effect of Different Representations of Wind Turbines on the SSR Analysis in the Double Cage Induction Generator Based Wind Farm. *International Journal of Industrial Electronics, Control and Optimization*, 3(1), 69-80, 2020.

[3] H. Hajiabadi, M. Farshad & M. Shamsinejad, Multi-objective optimization and online control of switched reluctance generator for wind power application. *International Journal of Industrial Electronics Control and Optimization*, 4(1), 33-45, 2021.

[4] E. Jafari, coordinated operation of Wind Farms, Cascaded Hydro, Photo-voltaic and Pump-storage Units by WT-ANN-ICA Prediction Method. *International Journal of Industrial Electronics Control and Optimization*, 4(1), 127-139, 2021.

[5] J .L.Menet, N. Bourabaa, "Increase in the savonius rotor efficiency via α parametric investigation,", European Wind Energy conference & exhibition (pp. 22-25). Nov 2004.

[6] U.K. Saha, M.J.Rajkumar, "On the performance analysis of savonius rotor with twisted blades," *Renewable energy*, vol 31, pp: 1776-1788, 2006.

[7] N.H. Mahmoud, A.A. El-Haroun, E. Wahba, M.H. Nasef,, "An experimental study on improvement of Savonius rotor performance," *Alexandria Engineering Journal*, vol 51, pp:19–25, 2010.

[8] M. C. Percival, P. S. Leung, P. K. Datta, "The Development of a Vertical Turbine for Domestic Electricity Generation,", In European Wind Energy Conference (pp. 22-25). Nov, 2004.

[9] A. Abdlokadir, S.Golde. F.Alam. H. Maria, "Experimental and Computational Study of Micro Vertical Axis Wind Turbine," *IEF International Energy Congress*, vol 49, pp: 254-262, 2012.

[10] Saeed. Qodsi, M. Jamil, M. Layeqi, "Aerodynamic simulation of the wind turbine of Sovenius on the roof of the solar building of the Materials and Energy Research Center", *MSc Thesis, Iran Materials and Energy Research Institute*, 2014.

[11] Jaber Hossein Zadeh Geravi, Mehran Nosratollahi, Mostafa Mahmoudi, "Numerical and experimental study of the effect of coverage ratio on the performance of a domestic wind turbine," *Journal of Engineering and Energy Management*, 5(1), 54-53, 2015.

[12] Park, G. L., A. I. Schäfer, and B. S. Richards., "Potential of wind-powered renewable energy membrane systems for Ghana," Desalination 248.1-3, 169-176, 2009.

[13] Verma, Shivendra, Ramsingh Meena, and Anurag Mudgal., "A Cost-Effective Wind Power-Driven RO Plant for Treatment of Brackish Water," *Journal of Geoscience and Environment Protection* 3.10, 40, 2015.

[14] Alsairafi, A. A., and M. H. Al-Shehaima., "Wind Driven Reverse Osmosis Desalination for Concrete Factory Application in Kuwait," *Journal of Clean Energy Technologies* 4.2, 2016.

[15] Maeda, M., & Watts, D., "The unnoticed impact of long-term cost information on wind farms," economic value in the USA. –A real option analysis', Applied energy, 241, 540-547, 2019.

[16] Muhammad Yavari Foroushani, Mohammad Javad Mehrani, "The feasibility study of the use of Sovenius wind micro-turbine in roof of residential buildings in Tehran," *National Energy Conference, Islamic Azad University, Khomeini Shahr Branch*, 2015.

[17] Kaewchoothong, N., & Nuntadusit, C. Flow and Heat Transfer Behaviors in a Two-Pass Rotating Channel with Rib Turbulators using Computational Fluid Dynamics, Heat Transfer Engineering, 1-19. Feb 2022.

[18] O. Rabaza, D. G, M. J. Mercado-Vargas, D. Gómez-Lorente, O. Rabaza, and E. Alameda-Hernandez, "Aggregated models of PMSG wind farms," *Renew. Energy*, vol. 83, pp. 1287–1298, 2015.

[19] S. Das, & O. H. Gupta, Study and Simulation of a PMSG-Based Wind Turbine, Recent Advances in Power Electronics and Drives, Springer, pp. 37-46, 2021.

[20] H. Khosravi, M. Jamil, "Effect of aerodynamic, positioning and number of advanced Savonius rotor blades on efficiency and torque of wind turbine," *MSc Thesis, Iranian Institute of Materials and Energy*, 2011

[21] M.Prakash, & J. Young-Hoon, "Fuzzy Event-triggered Control for Back to Back Converter involved PMSG-based Wind Turbine Systems." IEEE Transactions on Fuzzy Systems, 2021.




**Hassan Zare** received his Ph.D. from Semnan University, Iran in 2018. He is currently an Assistant Professor with Technical and Vocational University (TVU), Tehran, Iran. His research interests include power system stability and control, electrical machines and drive, converters, and their application in renewable energy.



**Alireza Nateghi** was born in Tehran, Iran in 1969. He received his B.Sc. degree from the Sharif University of Technology, Tehran, Iran in 1999. He received his M.Sc. and Ph.D. degrees in Electrical Engineering from Shahid Beheshti University, Tehran, Iran in 2009. He joined the University of Shahid Sattari as an Assistant Professor in the Department of Electric Engineering, from 2010 to 2021. His current research interests include control of distributed energy resources and design and control of power electronic converters for microgrids**.**



**Hossein Asgharpour-Alamdari** received his Ph.D. from Semnan University, Iran in 2017. He is currently an Assistant Professor with Technical and Vocational University (TVU), Tehran, Iran. His research interests are power system stability and control, power system protection, electrical machines, and their application in renewable energy.

IECO

This page intentionally left blank.